THE ASTROPHYSICAL JOURNAL, 451:167–175, 1995 September 20

INTERNAL HEATING OF MOLECULAR CLOUDS BY TIDAL FIELDS

MOUSUMI DAS & CHANDA J. JOG
Joint Astronomy Programme, Department of Physics, Indian Institute of Science, Bangalore 560012, India
Received 1994 October 17; accepted 1995 March 28

ABSTRACT

We present a study of the effect of the galactic tidal field on the internal energy of molecular clouds, moving in the disk or central bar potential of a galaxy. During epicyclic motion or obtital motion in a bar, the tidal field across a cloud varies with time. This time variation of the tidal field across the cloud couples the rotational motion in the galaxy to the internal clump motion within the cloud. There will be a net exchange of internal energy between the cloud and the external gravitational field of the galaxy. We have examined this effect to see whether tidal fields are an important heating mechanism for molecular clouds and hence important for cloud support.

An N-body simulation method has been used to treat the motion of clumps in molecular clouds. A cloud is initially virialized in a circular orbit to obtain a relaxed, clumpy system having a centrally peaked mass profile. The clouds were then evolved in epicyclic orbits and also closed orbits in a nonaxisymmetric bar potential.

We find that the heating effect of the tidal field is not important for epicyclic motion, but it is significant for a cloud moving in a bar potential. For a cloud of mass $5 \times 10^4\ M_\odot$, the change in internal energy is 10%–15% of the initial internal energy. Thus, although tidal fields alone cannot provide the energy required for cloud support, their contribution is significant in a bar potential. Also, some clumps become unbound from the cloud during the bar orbits. This can explain the origin of diffuse molecular gas which has been observed in the central regions of galaxies like our Galaxy, IC 342, and NGC 1808. We also find that an initially virialized cloud is not disrupted by the tidal field after a few rotations in the bar potential.

Subject headings: galaxies: kinematics and dynamics — ISM: clouds — ISM: kinematics and dynamics — ISM: molecules

1. INTRODUCTION

The first large-scale surveys of molecular gas in the Galaxy indicated that molecular clouds are an important component of the interstellar medium. They constitute $\sim 50\%$ of the interstellar gas mass (e.g., Scoville & Sanders 1987). They are the sites of star formation. It has been observed since the late 1970s that molecular clouds are highly inhomogeneous and have substantial substructure (e.g., Barrett, Ho, & Myers 1977). The clouds have large envelopes of neutral gas and contain dense clumps of molecular gas moving in a low-density interclump medium. The clump-interclump density contrast is high (10–100), and the clumps contain a large fraction (50%–90%) of the cloud mass (e.g., Blitz 1991; Genzel 1992).

It is well known that a typical molecular cloud in the Galaxy, although gravitationally bound, does not appear to be in a free-fall collapse. This is deduced from the small rate of star formation. At the mean observed gas densities the gravitational free-fall collapse time for molecular clouds is $\approx 10^6$ yr, and the total molecular mass in the Galactic disk is $\approx 2 \times 10^9\ M_\odot$. Hence, the expected star formation rate (SFR) in the Galaxy is $\approx 10^3\ M_\odot\ \mathrm{yr}^{-1}$. However, the observed SFR is only a few $M_\odot\ \mathrm{yr}^{-1}$. This means that molecular clouds are not in a free-fall collapse (e.g., Solomon & Sanders 1980). A typical molecular cloud is observed to have large nonthermal line widths which are 5–10 times the thermal line widths (e.g., Scoville & Sanders 1987). This indicates that molecular clouds could be supported by internal random motions. Also, since the velocity dispersion in a cloud is proportional to the square root of the cloud diameter for a wide range of molecular masses, the clouds seem to be in virial equilibrium (Larson 1981). However, clump collisions are highly dissipative. Therefore, if a molecular cloud is to be supported by internal motions, there must be some large-scale source of energy which continuously replenishes the energy loss due to clump collisions. The energy loss takes place on a dynamical timescale $t_d \sim R/v$, where v is the average clump velocity and R is the cloud radius; $t_d \sim 10^5$–10^6 yr.

The origin of the nonthermal motions and hence the cloud support against gravitational collapse has been a long-standing problem. In the past, various mechanisms have been proposed to support the internal motions. Norman & Silk (1980) proposed that outflows from young stars could energize clump motions. However, many dark clouds which do not have young stars are found to have broad nonthermal line widths. The magnetic field must also be an important factor in cloud support. For example, Myers & Goodman (1988) have shown that for the clouds they observationally obtain, the velocity dispersion is proportional to the square root of the magnetic field and cloud diameter.

Another source of energy could be the rotation of the Galaxy itself. This has been suggested by Fleck (1980, 1981), who has given estimates for cloud internal heating, but based on dimensional arguments only. Wilson & Walmsley (1989) have suggested that the tidal field across a molecular cloud probably plays an important role in cloud support. Kenney & Lord (1991) have suggested that tidal forces can prevent cloud collapse in bars where tidal effects are larger. They propose that this may be a reason for low star formation efficiency in the bars of galaxies such as M83.

However, these papers have not given an explicit, physical mechanism to couple the large-scale rotational motion in a galaxy to the internal motion within a molecular cloud. This is

the main motivation for this work: to study the details of an internal support mechanism for molecular clouds. We propose that the time-dependent tidal field across a molecular cloud can couple the external rotational energy in a galaxy to the internal motion within a molecular cloud. This is the first time that a cloud support mechanism which links the rotational energy in a galaxy to the internal cloud energy has been studied in detail.

In this paper we have tried to see whether tidal fields can provide a steady internal heating to galactic molecular clouds. The tidal field across a molecular cloud varies during its motion in a bar potential and also during its epicyclic motion about a circular orbit. This time-dependent tidal field couples the large-scale gravitational forces to the internal clump motions. Thus, there is a net exchange of energy between the cloud and the external gravitational field. The ultimate energy source for this heating mechanism is the gravitational field of the galaxy. This is analogous to the steady internal heating of a planet by continuously varying tidal fields due to other planets and the Sun (e.g., Hubbard 1984, p. 75). However, molecular clouds are not elastic solids but clumpy systems, and so the details of the heating mechanism are different.

We have investigated the tidal heating due to motion in a bar potential and epicyclic motion in the Galactic disk and nucleus, assuming a nonbarred, azimuthally symmetric nuclear potential. Before discussing the detailed calculations, we will make a rough estimate to see how important the effect is. For a disk cloud, the tidal force is $t_f = 2Mv_c^2 D/R_g^2$, where M is the cloud mass, v_c is the rotation velocity, D is the cloud diameter, and R_g is the radius of the circular orbit. The tidal heating for a net distortion δx of the cloud is $\delta E \sim t_f \delta x$. Let the cloud execute $\frac{1}{4}$ of an epicyclic orbit, so that the orbital radius changes from R_g to $(R_g + A)$, A being the epicyclic amplitude. The diameter of a tidally stable cloud is $D = (2GMR_g^2/v_c^2)^{1/3}$. Hence, if a cloud is tidally stable at R_g and $(R_g + A)$, the net distortion $\delta x = 2/3(A/R_g)D$. The epicyclic period is $\sim 10^8$ yr. So the heating rate over $\frac{1}{4}$ epicyclic period is $\delta E/\delta t \sim 2.6 \times 10^{40}$ ergs yr^{-1}, where $M = 10^5\ M_\odot$, $v_c = 230$ km s^{-1}, $D = 75$ pc, $R_g = 5$ kpc, and $A = 80$ pc.

On the other hand, the heating rate for a cloud in a bar potential is larger. Let a cloud move in an elliptical orbit of axes ratio 0.75 and having semimajor axis $a = 1000$ pc. For a tidally stable cloud $D = (M/8M_T)^{1/3}R_0$, where M_T is approximately the central mass within the equipotential and R_0 is the radial distance to the center. The deformation of a cloud during $\frac{1}{4}$ of an orbital period during which it moves from $R_0 = 1000$ pc to 750 pc is $\delta x = 0.25D_0$, where D_0 is the cloud radius at $R_0 = 1000$ pc. The tidal force is $t_f = 2GMM_T D/R_0^3$. The mass within 1000 pc is taken as $M_T \sim 8 \times 10^9\ M_\odot$ (Binney et al. 1991), and the orbital period for an orbit of semimajor axis $a = 1000$ pc is $\sim 4 \times 10^7$ yr (see § 4.1). Hence, the tidal heating rate averaged over $\frac{1}{4}$ of an orbit for a cloud of mass $M = 10^5\ M_\odot$ is $\delta E/\delta t \sim 4.8 \times 10^{41}$ ergs yr^{-1}.

The dissipation rate in clouds due to inelastic collisions is $\sim 8.8 \times 10^{41}$ ergs yr^{-1} (Falgarone & Puget 1988). The tidal heating in the disk is $\sim 2.6 \times 10^{40}$ ergs yr^{-1}, and for the bar it is $\sim 4.8 \times 10^{41}$ ergs yr^{-1}. Hence, the above simple estimates indicate that tidal heating in a bar may be fairly important.

In the following sections, we study this cloud support mechanism in more detail. The above simple estimates do not take into account the internal structure of molecular clouds, and this is important in determining how much energy can be coupled to the internal motion within a cloud. Molecular clouds are observationally found to be virialized, self-gravitating systems having a centrally peaked mass profile (Sanders, Scoville, & Solomon 1985). It was thus necessary to treat them as clumpy, virialized systems, and so an N-body simulation technique was used to develop a realistic cloud model. This model was used to study the effect of the time-dependent tidal field on the internal energy of a cloud as it moves in an epicyclic orbit or in a bar potential in the Galaxy.

We find that the gain in energy is not significant for molecular clouds moving in an axisymmetric potential in the disk or in the central region of a nonbarred galaxy. Thus, the large-scale gravitational field is not an important contributor to cloud support in the disk region, where the time variation of the tidal field across the cloud is small. It is also not important for molecular clouds in the central, nonbarred region of a galaxy, since they are too dense to be heated by tidal fields. This null result for disk and nuclear molecular clouds is contrary to previous expectations that tidal shear is an important source of cloud internal energy.

We find that tidal fields are important for clouds moving in eccentric bar orbits where the tidal field across a cloud varies a great deal with time. It is large enough to produce a 10%–15% heating effect on a molecular cloud. Though this may not be enough to sustain internal cloud velocities, it is a fairly significant effect. Also, as a cloud moves in a bar orbit, it loses mass from the outer regions. A molecular cloud has a centrally peaked mass profile, and hence the clumps lying in the outer regions can be evaporated by the variation in the tidal field across the cloud. This can explain the origin of molecular intercloud gas (ICM) seen in the central regions of galaxies such as our Galaxy, IC 342, and NGC 1808.

Section 2 deals with the cloud parameters, the Galactic potential, and the bar potential used in the numerical calculations. The bar potential has been derived from a density distribution numerically (Binney et al. 1991), the details of which have been outlined in this section. A system of particles was viralized in the Galactic potential to obtain a clumpy cloud in virial equilibrium. This has also been discussed in § 2. In § 3, the effects of the time-dependent tidal field in the disk and nonbarred nuclear region have been studied. Section 4 deals with the effect of the time-dependent tidal field in a bar potential. A discussion of the results, their implications, and the limitations of the model is presented in § 5. We end with conclusions in § 6.

2. MODEL PARAMETERS

In this section we present the model of the cloud, the disk, and azimuthally symmetric nuclear potentials that we have used in the calculation. We also discuss the bar potential used in the numerical modeling.

2.1. *Cloud Model*

Our model of a molecular cloud assumes the following characteristics. A molecular cloud (i) is a clumpy system, (ii) has internal dissipation, and (iii) is close to virial equilibrium.

The cloud model assumed here is similar to the generalized model of a clumpy molecular complex suggested by Falgarone & Puget (1986). A cloud is composed of 200–1100 identical clumps; each clump having a mass of 270 $M_\odot$. Hence, the total cloud mass varies between 10^4 and $10^5\ M_\odot$ approximately. The disk simulations were performed with clouds of 200 and 1100 clumps (masses $5.4 \times 10^4\ M_\odot$ and $3 \times 10^5\ M_\odot$). For the bar potential, simulations were carried out with 200 and 800

clump clouds (masses $5.4 \times 10^4\ M_\odot$ and $2 \times 10^5\ M_\odot$). The small number was taken for numerical simplicity. These clouds are taken to represent the less massive and more massive clouds in the disk and bar, respectively. The number of clumps taken has no other significance.

In order to take account of internal dissipation within the clouds, the equation of motion for a clump contains a viscous damping term $\Gamma(\boldsymbol{v}_i - \boldsymbol{v})$ where $\boldsymbol{v}_i$ is the velocity of the ith clump, $\boldsymbol{v}$ is the mean velocity of the clumps in the cloud, and Γ is the damping coefficient. This is similar to the treatment of energy dissipation in clouds by Elmegreen (1992), where the cooling rate due to clump collisions leads to a cooling time $\tau \approx 2 \times 10^7$ yr. This corresponds to a $\Gamma \approx 0.5$. The value of Γ used in our simulations is of the same order. The clump collisions are thus taken to be dissipative but nonsticky, and hence do not affect the clump mass spectrum.

To satisfy the third criterion, a system of clumps was virialized in a constant circular orbit. This is described in detail in § 2.3.

2.2. *Galactic and Bar Potential*

The Galactic potential for the azimuthally symmetric disk and nucleus used in this problem is from Carlberg & Innanen (1987). They have determined a four-component potential which produces a flat rotation curve in which $v_\odot = 235$ km s^{-1} at $R_\odot = 8.5$ kpc. Since both R and Z epicyclic motions have been included in our simulations, it was important to have a disk-halo potential which also contained a spherical component.

The bar potential used in the problem is based on the modeling of the central mass distribution by Binney et al. (1991). From the observations of the central H I, CO, and CS emission, they have constructed a density distribution for the inner region which is generated by a prolate body having a density distribution of the form

$$\rho(a) = \rho_0\left(\frac{a_0}{a}\right)^{1.75} \qquad a \le a_0\ , \tag{1}$$

$$\rho(a) = \rho_0\left(\frac{a_0}{a}\right)^{3.5} \qquad a \ge a_0\ , \tag{2}$$

where a is the elliptic coordinate:

$$a^2 = x^2 + \frac{y^2 + z^2}{q^2}\ . \tag{3}$$

Since the orbits of the gas flow do not extend beyond 1.2 kpc, they have chosen $a_0 = 1.2$ kpc. The axis ratio $q = 0.75$ and $\rho_0 = 0.68\ M_0$ pc^{-3}. The cloud orbits in our simulation also do not extend beyond 1.2 kpc.

The bar represents a prolate body in which the isodensity surfaces are triaxial ellipsoids of constant m, where m is given by

$$m^2 = a_1^2\left(\frac{x^2}{a_1^2 + \tau} + \frac{y^2}{a_2^2 + \tau} + \frac{z^2}{a_3^2 + \tau}\right), \tag{4}$$

and τ labels the isopotential surfaces. The gravitational potential of the ellipsoid is calculated by breaking it into thin triaxial homoeoids. The potential is summed over these homoeoids (Binney & Tremaine 1987):

$$\Phi = -\pi G\left(\frac{a_2 a_3}{a_1}\right)\int_0^\infty \frac{[\psi(\infty) - \psi(m)]d\tau}{\sqrt{(\tau + a_1^2)(\tau + a_2^2)(\tau + a_3^2)}}\ , \tag{5}$$

$$\psi(m) = \int_0^{m^2} \rho(m^2)dm^2\ . \tag{6}$$

The final form of the potential is

$$\Phi_b(x, y, z) = -\frac{28}{3}\pi G(a_1 a_2^2)\rho_0 \times \int_0^\infty \left[1 - \frac{6}{7}\left(\frac{x^2}{a_1^2 + \tau} + \frac{y^2}{a_2^2 + \tau} + \frac{z^2}{a_2^2 + \tau}\right)^{1/8}\right] \times [\sqrt{(\tau + a_1^2)(\tau + a_2^2)(\tau + a_2^2)}]^{-1}\, d\tau\ . \tag{7}$$

The integral has to be estimated numerically at a point to determine the potential at that point. To find the force at each point (x, y, z) in the bar potential, the derivative also has to be numerically estimated. For example, the force component along the x-axis is

$$F_x(x, y, z) = -2\pi G\rho_0(a_1 a_2^2)x \times \int_0^\infty \left(\frac{x^2}{a_1^2 + \tau} + \frac{y^2}{a_2^2 + \tau} + \frac{z^2}{a_3^2 + \tau}\right)^{-7/8} \times [(\tau + a_1^2)^{3/2}(\tau + a_2^2)]^{-1}\, d\tau\ . \tag{8}$$

In order to compare the energy of a cloud tidally heated in a bar potential to the energy of a cloud moving in constant circular orbit, an equivalent circular potential has to be determined. So at a radius r, an average of the bar potential over a path $2\pi r$ is calculated for $r = 0$–1.2 kpc. This potential Φ_{bc} represents an equivalent axisymmetric potential. The numerically determined potential Φ_{bc} is plotted against r and fitted with a polynomial. This polynomial is used to calculate the potential and force on a cloud moving in the equivalent circular orbit. The polynomial was taken up to the eighth degree. It was tested on a point particle and then used in the N-body simulation of a cloud of clumps.

2.3. *Virialization*

As mentioned in § 1, molecular clouds seem to be in virial equilibrium (e.g., Larson 1981). Hence, in our model the cloud was taken to be a relaxed, clumpy system. To obtain such a cloud in virial equilibrium, a system of particles (i.e., clumps) was randomly distributed within a sphere. The system was evolved in time under its internal gravitational forces and the external Galactic potential Φ. The particles are given a random Gaussian velocity distribution along each direction. The equation of motion for the ith clump is

$$\ddot{\boldsymbol{r}}_i = -\sum_j \frac{Gm(\boldsymbol{r}_i - \boldsymbol{r}_j)}{(|\boldsymbol{r}_i - \boldsymbol{r}_j|^2 + \epsilon^2)^{3/2}} - \nabla\Phi\ . \tag{9}$$

In our numerical modeling the clumps are taken as particles and the gravitational attraction is softened with ϵ, where ϵ is 10% of the radius of the initial distribution. This N-body treatment of a clumpy cloud is similar to the simulation of cloud ensembles in a spiral potential (e.g., Kwan & Valdes 1987; Tomisaka 1986). Though it is a simplification of the system, we feel it will give an estimate of the effect of the tidal forces on a molecular cloud.

The first term on the right-hand side of equation (9) is due to clump interactions and is calculated by summing over all the

clump pairs in the cloud. A very competent differential equation solver ODEN was used to evolve the equation of motion for each clump. The total random kinetic energy T and the self-gravity V of the cloud is calculated after every few iterations. The ratio of the averages $\langle T\rangle/\langle V\rangle$ is plotted against the time of relaxation (Fig. 1). After a few crossing times, the system relaxes, i.e., $\langle T\rangle/\langle V\rangle \approx 0.5$–1. The ratio is 0.5 for a Keplerian potential and 1 for a harmonic oscillator. During relaxation, the energy and angular momentum do not change by more than a few percent.

The above numerical procedure was carried out for both 1100 and 200 clump clouds virialized in circular orbits in the disk and the nuclear region for an azimuthally symmetric potential (§ 3). This was also done for 200 and 800 clump clouds in the equivalent circular orbit of a bar potential (§ 4). The unbound clumps were removed so that finally a bound, relaxed system of clumps remained. The final density profile of the cloud is always centrally peaked (Fig. 2). The velocity distribution obtained for the final cloud is Gaussian. The radius of the virialized cloud depends on the radius of the axisymmetric orbit. At larger radii in the disk, the final cloud size is greater than at smaller radii. This is simply because the tidal field across the cloud is smaller at larger radii.

For example, when a cloud of 200 clumps was virialized in the disk potential Φ_c at a Galactic radius of 5 kpc (Fig. 1), four clumps became unbound. The mass profile of the final relaxed, bound cloud is shown in Figure 2, where the cumulative number of clumps within a radius is plotted against the radial distance. The resulting centrally peaked profile is in good agreement with the observed profiles (e.g., Sanders et al. 1985). To calculate the mean density we took the radius within which approximately half the cloud mass is contained. For example, for a disk cloud of ~200 clumps, half the mass is within a radius of 10 pc. This leads to a mean number density $n_c \sim 150$ cm^{-3}. The internal one-dimensional velocity dispersion for the clumps within the virialized cloud is $\sigma_{1d} \approx 1.8$ km s^{-1}. For the bar region, a 200 clump cloud has $n_c \sim 2 \times 10^4$ cm^{-3}, and a large cloud of 800 clumps has $n_c \sim 10^4$ cm^{-3}. The corresponding internal velocity dispersion for the large cloud is $\sigma_{1d} \approx 5.7$ km s^{-1} and for the small cloud it is $\sigma_{1d} \approx 3.4$ km s^{-1}. These values for the number density and internal velocity dispersions are of the same order as the corresponding observed values (Scoville & Sanders 1987; Genzel 1992). Thus, the cloud parameters used here represent real clouds fairly well, and therefore the results obtained should be applicable for molecular clouds in the Galaxy.

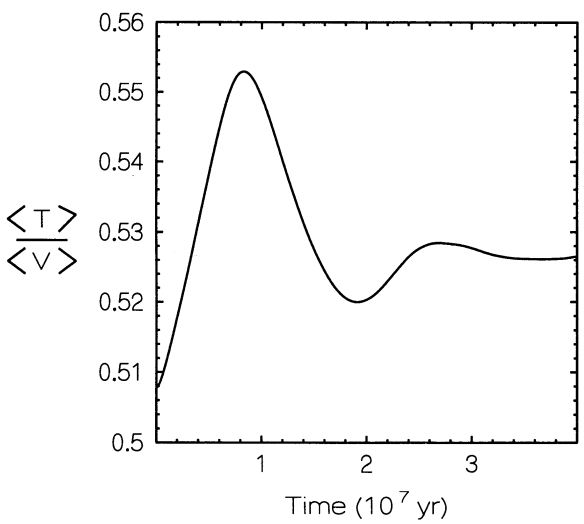

FIG. 1.—A plot against time of the ratio of the time-averaged random kinetic energy and gravitational potential energy within a molecular cloud of 200 clumps ($M \sim 5 \times 10^4\ M_\odot$). The system is evolved along a circular orbit of radius 5 kpc in the disk potential Φ_c; the flattening of the curve indicates that the system has relaxed.

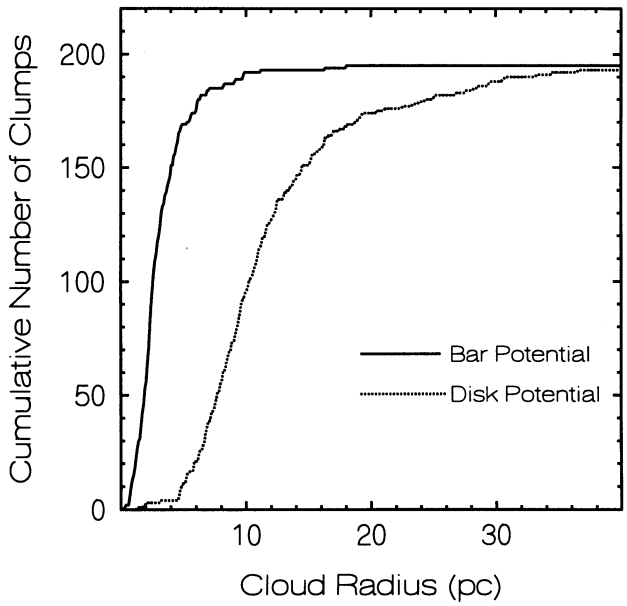

FIG. 2.—Mass profiles of the resultant virialized cloud in the central potential Φ_{bc} and in the disk potential Φ_c. The mass density of the cloud in the central potential is much more centrally peaked.

3. TIDAL HEATING FROM EPICYCLIC MOTION

A cloud moving in the axisymmetric Galactic potential has a certain amount of random motion along with rotational motion. In the epicyclic approximation, this can be considered as an oscillation about a stable circular orbit. During this epicyclic motion, the tidal force across the cloud varies with time. In the following sections we discuss the heating effect which is due to this time-dependent force on the cloud.

3.1. *The Equations of Motion*

The equation of motion of a clump in the cloud moving in the disk potential Φ_c is

$$\ddot{\boldsymbol{r}}_i + \Gamma(\dot{\boldsymbol{r}}_i - \dot{\boldsymbol{r}}) + \sum_j \frac{Gm(\boldsymbol{r}_i - \boldsymbol{r}_j)}{(|\boldsymbol{r}_i - \boldsymbol{r}_j|^2 + \epsilon^2)^{3/2}} = -(\nabla\Phi_c)_{\boldsymbol{r}_i}, \quad (10)$$

where $\boldsymbol{r}$ is the center of mass of the cloud, $\boldsymbol{r}_i$ is the position of the ith clump, and m is the mass of a clump. The Galactic potential Φ_c is from Carlberg & Innanen (1987). The right-hand side of the equation represents the gravitational field at $\boldsymbol{r}_i$. The internal dissipation has been assumed to be proportional to the random velocity of a clump, the constant of proportionality being Γ. This damping parameter represents the energy loss which is due to clump collisions and clump-interclump medium drag.

The cloud is evolved in an inertial frame whose origin is the Galactic center. To set the cloud into epicyclic motion, the

cloud is given an initial radial and vertical velocity along the x- and z-directions. The initial velocity along the y-direction is the rotational velocity v_c, which is determined from the potential Φ_c. To compare the effect of a time-dependent tidal field on a cloud to a constant tidal field, a virialized cloud is also evolved in a constant circular orbit of the same radius.

3.2. *Epicyclic Motion in the Disk*

For a cloud moving in an epicyclic orbit, the oscillation about a mean guiding center orbit can be represented by $R_0 = (R_g + A_r \cos \kappa t)$ and $Z_0 = A_z \cos (\nu t + \psi)$, where κ and ν are the epicyclic frequencies along the radial and vertical directions. Using the Carlberg & Innanen (1987) potential

$$\kappa^2 = \left(\frac{\partial^2 \Phi_c}{\partial R^2} + \frac{3L_z^2}{R^4}\right)_{R_g}, \tag{11}$$

$$\nu^2 = \frac{41.19}{(R_g^2 + 74.16)^{0.75}}, \tag{12}$$

where $L_z = v_c r$, v_c is the rotation velocity and R_g is the radius of the circular orbit in kiloparsecs. The radial epicyclic amplitude A_r is determined from the planar cloud-cloud random velocity v_{1d} (Jog & Ostriker 1988). The vertical epicyclic amplitude is obtained from the z-distribution of molecular clouds (Scoville et al. 1987):

$$A_r = \frac{\sqrt{2} v_{1d}}{\kappa \sqrt{1 + (\kappa^2/4\omega^2)}}, \tag{13}$$

$$A_z = 50 \left(\frac{M_{vir}}{10^5\ M_\odot}\right)^{-0.4} \text{pc}, \tag{14}$$

where ω is the rotational frequency and M_{vir} is the mass of the molecular cloud. To start the cloud in an epicyclic motion, initial radial and vertical velocities $v_r = A_r \kappa$ and $v_z = A_z \nu$ are given to the cloud along the x- and z-directions in addition to its circular velocity v_c along the y-direction.

3.3. *Numerical Procedure*

To determine the tidal heating of a cloud in epicyclic motion, a virialized cloud of clumps has to be constructed (§ 2.3). This involves some trial and error, since the cloud has to be dense enough to withstand the disruptive effect of the tidal force. The system expands and oscillates before finally coming into equilibrium. For example, 1100 particles were distributed in a sphere of radius 25 pc at a Galactic radius of 5 kpc. The system was relaxed by evolving it in a circular orbit until $\langle T \rangle / \langle V \rangle \approx 0.5$. About 20 particles became unbound, and they were excluded from the final cloud model.

Clouds are virialized along circular orbits in the disk at radii 5 kpc, 9 kpc, and 13 kpc to study the effect of radial position on the tidal heating of a cloud. These radii represent the behavior of molecular gas close to the peak of the molecular ring, at the solar radius, and in the outer parts of the disk. They are then evolved along circular and epicyclic orbits with internal damping to see the effect of the time-dependent tidal field. The one-dimensional cloud-cloud random velocity is assumed to be 5 km s^{-1}. At the Galactic radius of 5 kpc, a larger cloud of 1100 clumps is evolved to see the effect of cloud size on the tidal heating. Also, the random velocity is increased to 10 km s^{-1} to see if the change in amplitude has any effect on the tidal heating. The damping constant Γ is changed also. In each case, the total internal energy and the self-gravitational energy of the cloud are plotted with time to determine if there is any energy exchange. However, no significant tidal heating was observed in any of the above cases, i.e., the change was less than 1% of the initial cloud binding energy.

Therefore, we conclude from the above simulations that the time-varying tidal field due to epicyclic motion in the disk cannot impart any significant internal energy to a molecular cloud.

3.4. *Epicyclic Motion in the Central Region*

The simulation of a cloud in the central region of the Galaxy, assuming there is no bar, is similar to the way it is evolved in the disk. However, the epicyclic frequency is $\kappa = 2\omega$, as appropriate for a solid body rotation (Sanders 1989). In addition, the vertical and radial amplitudes are assumed to be due to cloud random velocities which are similar to the internal velocity dispersion of the clouds (Bally et al. 1988). Hence,

$$A_r = A_z = \frac{v_{1d}}{2v_c} R_g. \tag{15}$$

The internal one-dimensional velocity dispersion for a virialized cloud in the central region is set equal to the cloud random velocity i.e., $\sigma_{1d} = v_{1d}$. In the simulations, a small cloud virialized in a circular orbit of radius 800 pc has a velocity dispersion $\sigma_{1d} \sim 3.5$ km s^{-1}.

The rest of the numerical procedure is the same as for a disk cloud. A relaxed cloud is evolved in a circular and an epicyclic orbit with internal damping. However, no significant change in internal energy is seen, i.e., the change in energy is less than 1% of the initial value. This means that tidal heating is not important for azimuthally symmetric central potentials in galaxies.

3.5. *Results of Epicyclic Motion*

The time-dependent tidal field due to epicyclic motion in a nonbarred galaxy does not produce any significant change in the internal energy of a cloud. We have found this conclusion to remain unchanged for different values of the damping parameter, mass, and radial position in the Galaxy and larger values of the random velocity. Thus, the time-dependent tidal field in an axisymmetric galaxy does not contribute significantly to the internal energy of a molecular cloud.

4. TIDAL HEATING IN A BAR POTENTIAL

In this section we calculate the time-dependent tidal field on a cloud in a bar potential. The bar potential has been derived from the density distribution in § 2.2.

4.1. *Closed Orbits*

The potential and, hence, force on a particle in the bar potential can be obtained from equations (7) and (8). The orbit of a particle having a certain initial velocity can be evolved in the rotating frame of the bar potential. However, clouds will tend to follow only closed orbits in a bar potential. This is because the system of clouds is a dissipational system and so if the orbits are not closed, the clouds will collide and finally settle into closed orbits. Hence, we have first determined the closed orbits numerically and then evolved a cloud along a closed orbit.

The orbits are of two types (Fig. 3). They have been referred to as x_1 and x_2 orbits by Binney et al. (1991). The x_1 orbits lie along the major axis of the bar. The x_2 orbits are elongated perpendicular to the major axis; they lie deeper in the bar

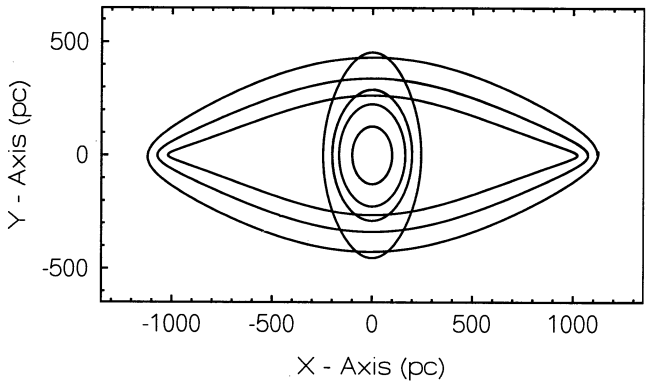

FIG. 3.—The closed orbits of a particle moving in a bar potential Φ_b rotating at a frequency $\omega = 63$ km s^{-1} kpc^{-1}.

potential than the x_1 orbits. There is a region between the x_1 and x_2 orbits where no closed orbits can be found. This region extends from approximately $x = 250$–1000 pc along the major axis.

4.2. *Equations of Motion*

The equation of motion of the ith clump of the cloud moving in the rotating frame of the bar is

$$\ddot{\boldsymbol{r}}_i = -\nabla\Phi_b - \Gamma(\boldsymbol{v}_i - \boldsymbol{v}) - \sum_j \frac{Gm(\boldsymbol{r}_i - \boldsymbol{r}_j)}{(|\boldsymbol{r}_i - \boldsymbol{r}_j|^2 + \epsilon^2)^{3/2}} - 2(\boldsymbol{\omega} \times \boldsymbol{r}_i) - (\boldsymbol{\omega} \times \boldsymbol{\omega} \times \boldsymbol{r}_i)\,, \quad (16)$$

where Φ_b is the bar potential and ω is the rotational speed of the bar; $\omega = 63$ km s^{-1} kpc^{-1} (Binney et al. 1991). The internal damping is proportional to the random velocity of the clump, i.e., $(\boldsymbol{v}_i - \boldsymbol{v})$, where v is the mean velocity of the clumps in a cloud.

For comparison, the same cloud is also evolved along an equivalent circular orbit. The equivalent axisymmetric potential Φ_{bc} is found by averaging the bar potential over a circumference for different radii (§ 2.2). The radius of the circular orbit is taken to be equal to the semiminor axis of the bar potential. The equation of motion of the ith clump in the cloud moving in an equivalent circular orbit is

$$\ddot{\boldsymbol{r}}_i = -\nabla\Phi_{bc} - \Gamma(\boldsymbol{v}_i - \boldsymbol{v}) - \sum_j \frac{Gm(\boldsymbol{r}_i - \boldsymbol{r}_j)}{(|\boldsymbol{r}_i - \boldsymbol{r}_j|^2 + \epsilon^2)^{3/2}}\,. \quad (17)$$

4.3. *Numerical Procedure*

The numerical procedure is similar to the axisymmetric case (§ 3). A system of clumps is virialized in the equivalent axisymmetric potential Φ_{bc}. The cloud has to be dense enough to withstand the disruptive effect of the tidal force, and this involves some trial and error while choosing the size of the cloud. The equivalent circular orbit has a radius equal to the semiminor axis of the potential corresponding to the chosen orbit. So for an orbit having a semimajor axis of 1020 pc, the equivalent circular orbit radius is 765 pc, since the bar potential has an axis ratio of 0.75 (Binney et al. 1991). We have evolved a cloud of 200 clumps and also a cloud of 800 clumps along the innermost x_1 orbit, which has a semimajor axis of length 1020 pc.

4.4. *Results of Cloud Motion in the Bar Potential*

We expect that the internal energy of a cloud moving in a closed orbit in the bar potential is not the same as that of a cloud moving in an equivalent axisymmetric potential Φ_{bc}. To examine this effect we have plotted the internal energy of a cloud of 200 clumps and 800 clumps as it changes with time. The internal energy is a sum of the internal random kinetic energy and potential energy of the bound system of clumps. The internal energy of the cloud is plotted against time for different values of the damping parameters (Figs. 4*a*, 4*b*, and 6).

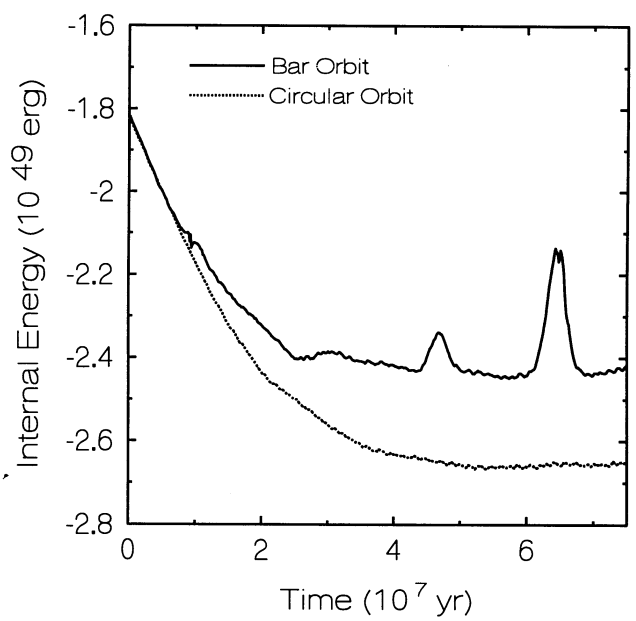

FIG. 4*a*

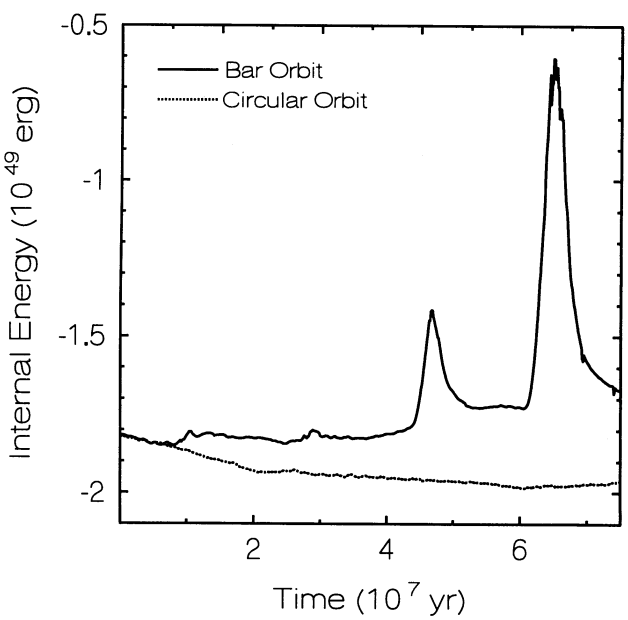

FIG. 4*b*

FIG. 4.—Plots against time of the internal energy of a bound cloud of ~200 clumps ($M \sim 5 \times 10^4\ M_\odot$) moving in a bar orbit and also an equivalent circular orbit, where the damping parameter Γ = (*a*) 0.2 and (*b*) 0.1. The tidal field yields a net average heating of ~12% of the initial internal cloud energy for $\Gamma = 0.2$ and 15% for $\Gamma = 0.1$.

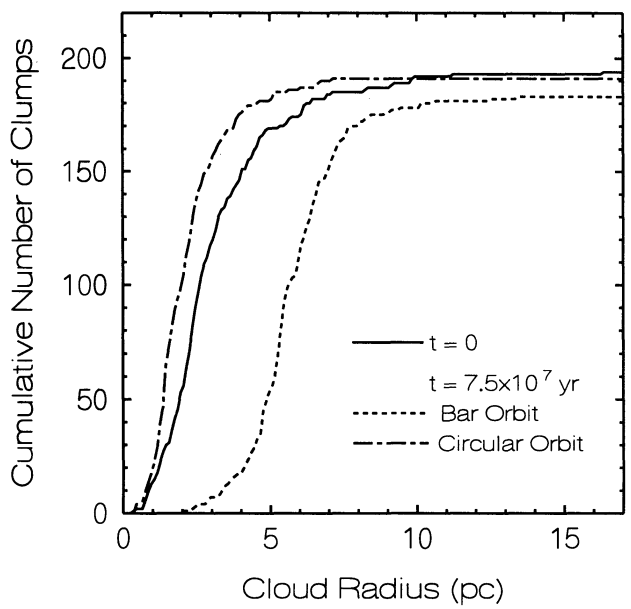

FIG. 5a

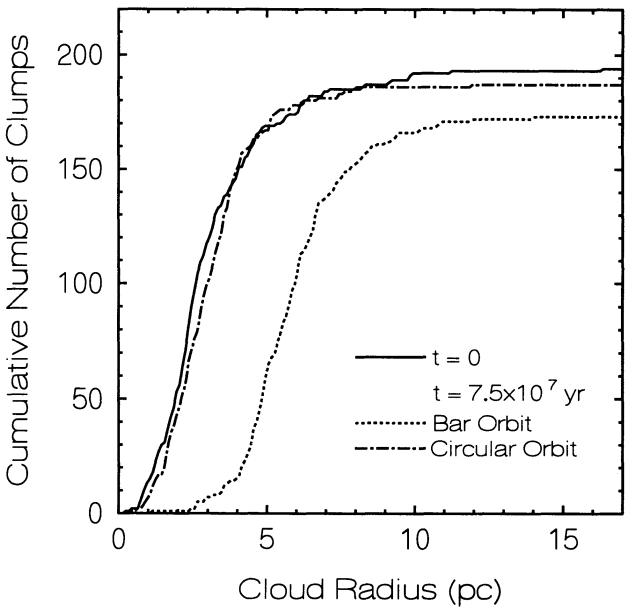

FIG. 5b

FIG. 5.—Initial and final mass profiles for a bound cloud of ~200 clumps ($M \sim 5 \times 10^4\ M_\odot$) moving in a bar orbit and an equivalent circular orbit, for (*a*) $\Gamma = 0.2$ and (*b*) $\Gamma = 0.1$. The cloud density decreases and it loses ~6% of its initial mass in two orbital periods for $\Gamma = 0.2$ and ~14.5% for $\Gamma = 0.1$.

During evolution, some clumps become unbound from the cloud. These have not been included in calculating the internal energy of the clouds. To see the effect of the tidal field on the density, we have also plotted the mass profile of a cloud after a time interval equal to two revolutions in the bar; for both a bar orbit and a circular orbit along with the initial cloud mass profile (Figs. 5*a*–5*b*). These figures show the cumulative number of clumps against the radial distance within a cloud. The period of the closed orbit is $\sim 3.6 \times 10^7$ yr. The results are described in detail below.

(i) *Internal Energy.*—As a cloud with internal damping is evolved in time, it slowly collapses. However, at any given time the internal energy of a cloud moving in a bar orbit is larger than in a circular orbit (Fig. 4) indicating that a cloud gains additional energy input through tidal fields in a bar potential. Thus, the time-dependent tidal fields on a cloud in a bar potential slow cloud collapse and perhaps inhibit star formation. This can explain the low star formation rate along bars (Kenney & Lord 1991). The internal energy for a cloud in a bar orbit also shows peaks near the regions of closest approach to the Galactic center (Fig. 4). This is because these are also the regions where a cloud experiences the largest tidal field in the orbit. The height of the peaks increases with time, indicating that as the number of revolutions increases a cloud becomes more susceptible to the effect of the tidal field. Hence, the cloud density must decrease with time as well. This is confirmed by the cloud mass profiles shown for $t = 0$ and $t = 7.5 \times 10^7$ yr (Fig. 5).

(ii) *Dependence on* Γ.—The tidal heating seems most pronounced for $0.1 < \Gamma < 0.3$. For $\Gamma < 0.1$, the cloud collapse is not pronounced, and hence this value does not seem a meaningful measure of internal dissipation. For $\Gamma > 0.3$, the heating effect does not seem significant. These values of Γ correspond to dissipation timescales of approximately $3–10 \times 10^7$ yr. For $\Gamma = 0.2$ (Fig. 4*a*), a 200 clump system shows an average change in internal energy of $\approx 12\%$ of the initial binding energy. For $\Gamma = 0.1$ (Fig. 4*b*), the difference is about 7% after one orbital period and increases to $\approx 15\%$ after two orbital periods. The peaks are also far more pronounced for a smaller value of Γ, indicating that a cloud with lower internal dissipation will be more tidally heated in a bar potential. The dependence of internal heating on Γ leads one to conclude that molecular clouds in bars having low internal dissipation are more prone to tidal heating and evaporation than highly damped clouds. However, since Γ corresponds to cooling timescales as $\tau \sim \Gamma^{-1}$ and clump collisions give a cooling time of a few times 10^7 yr (Elmegreen 1992), $\Gamma = 0.2$ is probably a good value to use in calculating the tidal heating for small molecular clouds in a bar potential. For $\Gamma = 0.2$, the tidal heating is only about 12% of the initial cloud binding energy. This is not as large as expected from the rough estimates in § 1. This may be because in the simple calculations we have considered a molecular cloud to be a continuous system, but it is actually a clumpy system with a centrally peaked density profile.

(iii) *Clump Evaporation.*—As a cloud starts collapsing in a bar or an axisymmetric potential, a few clumps become unbound, i.e., they evaporate from the cloud. However, the number of clumps lost by a cloud in a bar orbit is greater than in a circular orbit. For example, for a 200 clump cloud with $\Gamma = 0.2$ at $t = 7.5 \times 10^7$ yr, 12 clumps become unbound from the cloud moving in a bar orbit, but only four clumps evaporate from a cloud in circular orbit. For $\Gamma = 0.1$, 28 clumps are removed in a bar orbit, but only eight are removed from a cloud in circular orbit. This indicates that molecular clouds lose mass as they move in bar orbits. Hence, the bars of galaxies should contain some gas fraction in the form of small clumps of molecular or neutral gas, which forms part of the intercloud medium between dense clouds. This can explain the origin of such gas seen in a few galaxies such as our Galaxy (Bally et al. 1988), IC 342 (Downes et al. 1992), and NGC 1808 (Aalto et al. 1994).

(iv) *Cloud Density.*—Figure 5 shows the mass profile of small and large clouds for $\Gamma = 0.1$ and 0.2. The mass profile will be steeper and more centrally peaked for a denser cloud.

After two revolutions in a bar, the mass profile is less steep, indicating that a cloud becomes less dense as a result of the tidal field. Also, the mass profile saturates at a lower value than initially, the difference being due to the evaporation of clumps from the cloud.

(v) *Cloud Initial Position.*—The figures showing the effect of tidal heating on internal energy are the result of evolution begun at the end of the semimajor axis of the elliptical planar orbit at a distance of 1020 pc from the Galactic center. If the evolutions are begun at the tip of the semiminor axis, i.e., at 264 pc from the Galactic center, the results are qualitatively similar. The internal energy peaks always occur at distances of closest approach to the Galactic center where the tidal field is the greatest.

(vi) *Dependence on Cloud Mass.*—A cloud of 800 clumps having a total mass $M \sim 2 \times 10^5\ M_\odot$ was also evolved in the same bar orbit to see how the tidal heating effect changes with cloud mass. The tidal heating effect is surprisingly small for a large mass cloud and is never larger than 3% of the initial energy (Fig. 6). The heating does not noticeably change by varying Γ. The clump evaporation rate is also lower. For example, for $\Gamma = 0.1$, a large mass cloud loses only 20 clumps in two orbital periods ($\sim$2.5%), whereas a small cloud loses 28 clouds (14%). Since both clouds seem to have similar densities but different velocity dispersions, the reason must be that the massive cloud has a shorter internal relaxation time due to the greater internal random velocity. So the internal energy is dissipated away very quickly through clump collisions, and hence there is no net dynamical heating in the cloud. However, the energy may remain as thermal energy trapped in the cloud. Thus, tidal heating in bars is probably not important for clouds of mass larger than $10^5\ M_\odot$.

(vii) *Tidal Disruption.*—In our simulations we have evolved a virialized cloud in a bar orbit. Such a cloud is dense and hence not disrupted by the tidal field, though it does lose mass by clump evaporation. Hence, tidal disruption is not important for dense clouds moving in bars but may be important for clouds entering a bar from the disk region. Thus, the tidal disruption of incoming clouds may lead to the buildup of diffuse gas in a bar, depending on cloud densities, whereas gas shocking and cooling should lead to the buildup of dense clouds in a bar.

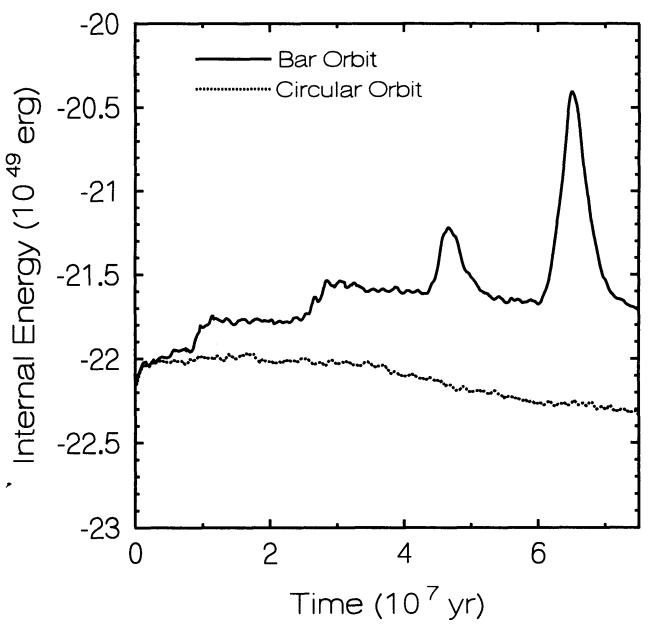

FIG. 6.—Plots against time of the internal energy of a bound cloud of $\sim$800 clumps ($M \sim 2 \times 10^5\ M_\odot$) moving in a bar orbit and also an equivalent circular orbit, where the damping parameter $\Gamma = 0.1$. The tidal field yields a net average heating of $\sim$3% of the initial internal cloud energy. This is much less than the internal heating of a smaller cloud of mass $\sim 5 \times 10^4\ M_\odot$.

5. DISCUSSION

Here we discuss some general points as well as the limitations of the present model.

1. We have used an N-body approach to model the clumpy structure of molecular clouds. The clumps have been assumed to be identical in size and mass and have been treated as point masses held together by their mutual gravitational attraction. This approach has been adopted for simplicity. A more realistic model would include unequal mass clumps moving in an interclump medium.

2. The internal dissipation in a cloud arises as a result of both clump collisions and clump-interclump medium drag. We have not modeled either phenomenon in detail. Also, Γ is actually a time-dependent quantity, changing as the internal structure of the cloud changes. Instead, the internal dissipation has been represented by a parameter Γ so that the rate of energy lost by a clump is Γv^2 and the deceleration is $-\Gamma v$. This is similar to the treatment of internal dissipation by Elmegreen (1992). We have adopted this simplified, dimensional appraoch for simplicity. We believe that the main results will hold even with these approximations.

3. To study the effect of the tidal field on a disk cloud at various radii in the disk, a cloud of particles was virialized at radii 5 kpc, 9 kpc, and 13 kpc. At larger radial distances, the virialized cloud becomes progressively larger in size. This indicates that the tidal field across a cloud decreases with increasing radial distance in the disk. This dependence of cloud size on radius has been observed in the Galaxy (e.g., Diegel, De Geus, & Thaddeus 1994).

4. We have used a virialized cloud to study the effect of the tidal field in the disk and in the central regions of galaxies. A real cloud may not be virialized and hence may not also have such a peaked density profile. In such cases the heating effect of the tidal field will be much stronger. Hence the present results may be a lower estimate of the heating effect of the tidal field.

6. CONCLUSIONS

We have studied the dynamical heating effect of tidal fields on molecular clouds in galaxies. Tidal fields provide a mechanism for coupling the rotational energy in the galaxy to the internal motion within a cloud. This is the first time that the detailed coupling mechanism has been studied. We find that the tidal heating caused by epicyclic motion in the disk or nucleus of a nonbarred galaxy is not significant. This is contrary to previous expectations that tidal shear is an important source of internal energy. Tidal fields are, however, a significant dynamical heating source for clouds moving in bar potentials and can provide $\sim$10%–15% of the cloud internal energy. This internal heating would be higher in a galaxy with a strong bar. However, the long-term support of molecular clouds must be caused by some other processes. For example, magnetic fields have been neglected in the present problem, but they

could well be the most dominant force in the gravitational stability of molecular clouds (e.g., Falgarone & Puget 1988). We also find that during the evolution of a cloud under tidal fields in a bar, some clumps become unbound from the cloud. This can qualitatively explain the origin of diffuse molecular gas found in the central regions of galaxies such as our Galaxy, IC 342, and NGC 1808.

M. D. would like to thank Rajaram Nityananda for discussions and valuable suggestions throughout the course of this work. She would also like to thank J. P. Ostriker and M. Valluri for suggestions regarding the bar potential. This work is part of the thesis work of M. D. and was supported by a research grant from CSIR, India [award number 9/79(269)/89-EMRI].

REFERENCES

Aalto, S., Booth, R. S., Black, J. H., Koribalski, B., & Wielebinski, R. 1994, A&A, 286, 365
Bally, J., Stark, A. A., Wilson, R. W., & Henkel, C. 1988, ApJ, 324, 223
Barrett, A. H., Ho, P. T. P., & Myers, P. C. 1977, ApJ, 211, L39
Binney, J., Gerhard, O. E., Stark, A. A., Bally, J., & Uchida, K. I. 1991, ApJ, 252, 210
Binney, J., & Tremaine, S. 1987, Galactic Dynamics (Princeton: Princeton Univ. Press)
Blitz, L. 1991, in The Physics of Star Formation and Early Stellar Evolution, ed. C. J. Lada & N. D. Kylafis (Dordrecht: Kluwer), 3
Carlberg, R. G., & Innanen, K. A. 1987, AJ, 94(3), 666
Diegel, S., De Geus, E., & Thaddeus, P. 1994, ApJ, 422, 92
Downes, D., Radford, S. J. E., Guilloteau, S., Guelin, M., Greve, A., & Morris, D. 1992, A&A, 262, 424
Elmegreen, 1992, in The Galactic Interstellar Medium, ed. D. Pfenniger & P. Bartholdi (New York: Springer), 157
Falgarone, E., & Puget, J. L. 1986, A&A, 162, 235
———. 1988, in Galactic and Extragalactic Star Formation, ed. R. E. Pudritz & M. Fich (Dordrecht: Kluwer), 195
Fleck, R. C. 1980, ApJ, 242, 1019
———. 1981, ApJ, 246, L151
Genzel, R. 1992, in The Galactic Interstellar Medium, ed. W. B. Burton, B. G. Elmegreen, & R. Genzel (New York: Springer), 379
Hubbard, W. B. 1984, Planetary Interiors (New York: Van Nostrand Reinhold)
Jog, C. J., & Ostriker, J. P. 1988, ApJ, 328, 404
Kenney, J. D. P., & Lord, S. D. 1991, ApJ, 381, 118
Kwan, J., & Valdes, F. 1987, ApJ, 315, 92
Larson, R. B. 1981, MNRAS, 194, 809
Myers, P. C., & Goodman, A. A. 1988, ApJ, 329, 392
Norman, C., & Silk, J. 1980, ApJ, 238, 158
Sanders, D. B., Scoville, N. Z., & Solomon, P. M. 1985, ApJ, 289, 373
Sanders, R. H. 1989, in IAU Symp. 136, The Center of the Galaxy, ed. M. Morris (Dordrecht: Kluwer), 77
Solomon, P. M., & Sanders, D. B. 1980, in Giant Molecular Clouds in the Galaxy, ed. P. M. Solomon & M. G. Edmunds (Oxford: Pergamon), 41
Scoville, N. Z., & Sanders, D. B. 1987, in Interstellar Processes, ed. D. J. Hollenbach & H. A. Thronson (Dordrecht: Reidel), 21
Scoville, N. Z., Yun, M. S., Clemens, D. P., Sanders, D. B., & Walker, W. H. 1987, ApJS, 63, 821
Tomisaka, K. 1986, PASJ, 38, 95
Wilson, T. L., & Walmsley, C. M. 1989, A&A Rev., 1, 141